Structure and Physical Properties of Cellulose Acetate Butyrate/Poly(butylene succinate) Blend

Tohru Tatsushima, Nobuo Ogata, Koji Nakane, Takashi Ogihara

Department of Materials Science and Engineering, Fukui University, 3–9-1 Bunkyo, Fukui 910-8507, Japan

Received 5 March 2004; accepted 1 August 2004
DOI 10.1002/app.21451
Published online in Wiley InterScience (www.interscience.wiley.com).

ABSTRACT: Cellulose acetate butyrate (CAB)/ poly(butylene succinate) (PBS) blend films were prepared by using a cast blend method with chloroform. Homogenous blend films were obtained over a wide range of the blend ratio. The compatibility and physical properties of the blends have been investigated. The following conclusions were deduced: i) CAB molecules inhibit crystallization of PBS in the blends; ii) over the range of PBS contents from 0 to 30 wt %, PBS molecules have a high miscibility with CAB molecules and PBS molecules are in an amorphous state; iii) over the range of PBS contents from 30 to 80 wt %, PBS molecules form both crystalline and amorphous regions, and a portion of the amorphous PBS molecules is blended with CAB molecules; iv) porous material could be obtained by immersing the blend films in acetone. © 2005 Wiley Periodicals, Inc. J Appl Polym Sci 96: 400–406, 2005

Key words: biodegradable; blends; differential scanning calorimetry (DSC); mechanical properties

INTRODUCTION

Amid the growing interest in global environmental issues, biodegradable polymers attract a great deal attraction not only as a solution to the plastic waste disposal problem, but also as an effective use of biomass. Because biodegradable polymers are degraded in the natural environment, many biodegradable polymers are produced from the biomass of agricultural products, wood chips, microorganisms, and so on. Cellulose is a promising material, especially from the viewpoint of the effective utilization of biomass, because cellulose is produced abundantly in nature; it is known that over 100 billion tons of cellulose is generated on the earth every year. However, cellulose also has the drawback that it is not suitable for the fabrication because it lacks thermal plasticity. Therefore, cellulose ester, the softening temperature of which is lowered by the addition of a plasticizer, is more commonly used in the industrial field. Cellulose acetate (CA), cellulose triacetate (CTA), and cellulose acetate propionate (CAP) are known as cellulose esters, which are frequently used.

A large number of studies have been made on the cellulose ester/biodegradable aliphatic polyester blend to increase the applicability of biodegradable polymers.[1–7] This research has suggested that the polymer blend expands the range of physical properties of biodegradable polymers. Some studies reported on the influence of molecular structures on the miscibility of the blend system. For example, Nishio et al.[5] studied the relation between the ability of cellulose ester derivatives to form a miscible blend with poly(caprolactone) (PCL) and the ester structure in terms of the side-chain length and the degree of substitution (DS). They reported that it is possible to deduce that cellulose butyrate, the number of carbons in the acyl substitution is four, exhibits the highest miscibility with PCL. They also suggested that the miscibility of the cellulose ester of the blend systems is enhanced with the increase in DS. Buchanan et al.[7] studied the influence of the diol length of an aliphatic polymer on the blend miscibility. To probe the relation between the polyester structure and the blend miscibility in the blend consisting of CAP and aliphatic polyester, they prepared a series of polyesters containing C5 dicarboxylic acid and diol, which was systematically varied from C2 to C8. They suggested that the polyester prepared from C2 to C6 diol exhibited the miscibility with CAP, and the polyester prepared from C4 diol had the highest level of miscibility.

The purpose of the present article is to develop a new material, which has a sufficiently wide range of mechanical properties to meet the industry's demands, and to provide broad knowledge about the miscibility of the cellulose ester/biodegradable aliphatic polyester blend system. We chose a cellulose acetate butyrate (CAB)/poly(butylene succinate) (PBS) blend system for the experiment; PBS is a biodegradable aliphatic polyester consisting of a C4 diol[8], and CAB is the cellulose ester that has high DS and butyryl substitution. Thus, for the reasons mentioned

Correspondence to: N. Ogata (ogata@matse.fukui-u.ac.jp).

above, this PBS/CAB blend system is expected to exhibit good miscibility. Furthermore, owing to the great difference in the molecular structure between CAB and PBS, it is anticipated that the blend polymer would exhibit a wide range of mechanical properties by changing the blend ratio. Furthermore, we attempt to provide porous material by using the difference of solubility; acetone can dissolve CAB but cannot dissolve PBS. Concretely, CAB is eluted from the interior of the blends by immersing the blend film in acetone. The surface area of the blend films increases as their porosity increases. As a result, it is expected that the degradation of porous material is accelerated in the natural environment.

EXPERIMENTAL

Materials

The PBS pellets and PBS sheet were supplied by Showa High-Polymer Co., Ltd.(Tokyo, Japan; commercial name, Bionolle B1001). CAB powder was supplied by Kanto Kagaku Co., Ltd (Tokyo, Japan). The reagent grade of chloroform (Nacalai Tesque Inc., Japan) was used as a cosolvent of these polymers without further purification. Furthermore, the reagent grade of acetone (Nacalai Tesque Inc., Japan) was used for preparation of porous material.

Preparation of the blends

Specified amounts of PBS pellets and CAB powder were placed in a beaker; the total amount of these materials was 1.0 g. Chloroform (20–30 mL) was added to the beaker. After being stirred vigorously, the mixture became a homogeneous solution. The solution was cast in a glass Petri dish. After chloroform was vaporized at 50°C, homogeneous films of about 100 μm in thickness were obtained. The blend film containing a given amount of PBS will be referred to as $\phi_{PBS} = X$, where X represents the weight percentage of PBS in the blend. In addition, we used a commercial PBS sheet for the mechanical test, because pure PBS films having a smooth surface could not be obtained by using the cast-blend method.

Characterization of the blends

A transmittance test of the blend films were performed with a Shimadzu UV-2100 spectrometer; a wavelength of 500 nm was used. The X-ray diffraction curves of the blends were recorded by a Mac Science PM-20 with CuKα radiation.

Thermal property of the blends was measured by using a Shimadzu DSC-60 differential scanning calorimeter (DSC) at a heating rate of 10°C/min. We evaluated the melting point, T_m, and the heat of fusion, ΔH_m, from the maximum position of the endothermic peak and its area, respectively.

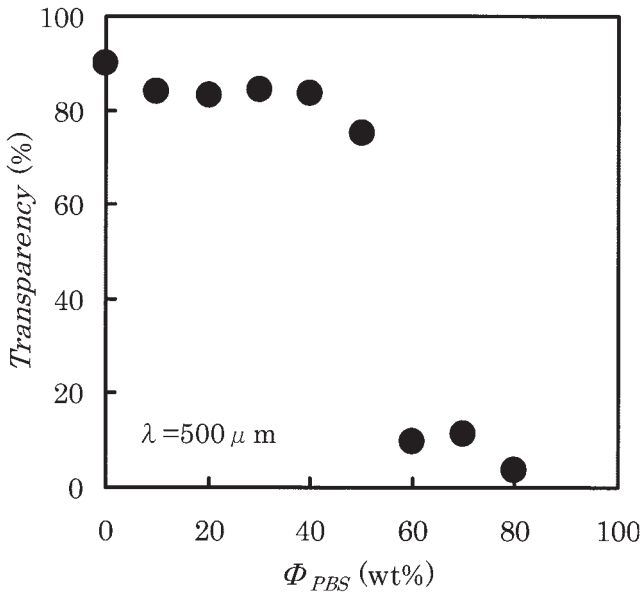

Figure 1 Effect of Φ_{PBS} on the transparency of the blend films.

Fourier transform infrared spectra (FT-IR) were recorded in the reflection mode by a Shimadzu model 8300 FT-IR spectrometer with the resolving power of 2 cm^{-1}.

Dynamic mechanical analyses (DMA) of the blends were performed with a Rheometric Scientific RSAII Viscoelastic Analyzer. Temperature scans at 1 Hz frequency were carried out with a heating rate of 2°C/min. The glass transition temperature, T_g, was evaluated from the peak position of the loss modulus (E'')versus temperature curve.

The tensile tests for the blends were performed at room temperature on a Tensilon UTM-II-20 tensile tester (Toyo Baldwin Co. Ltd.); the crosshead speed was 10 mm/min and the initial gauge length was 50 mm.

Preparation and observation of porous material

The blend film was immersed in acetone that was shaken at a constant speed. The samples were removed from acetone after 2 days. The samples were subjected to a scanning electron microscope (SEM, HITACHI S-2400) to observe the surface and the cross-sectional surface. Furthermore, we performed a DSC test to determine the effect of the immersion on the thermal property of blend films.

RESULTS AND DISSCUSSION

Structure and mechanical properties of the blends

Figure 1 shows the result of the light transmittance test. The transparency of the blend films is around

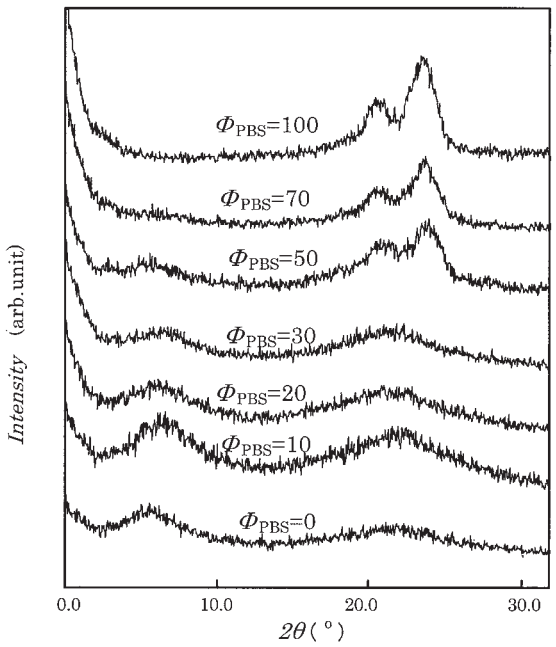

Figure 2 WAXS patterns for the blend films.

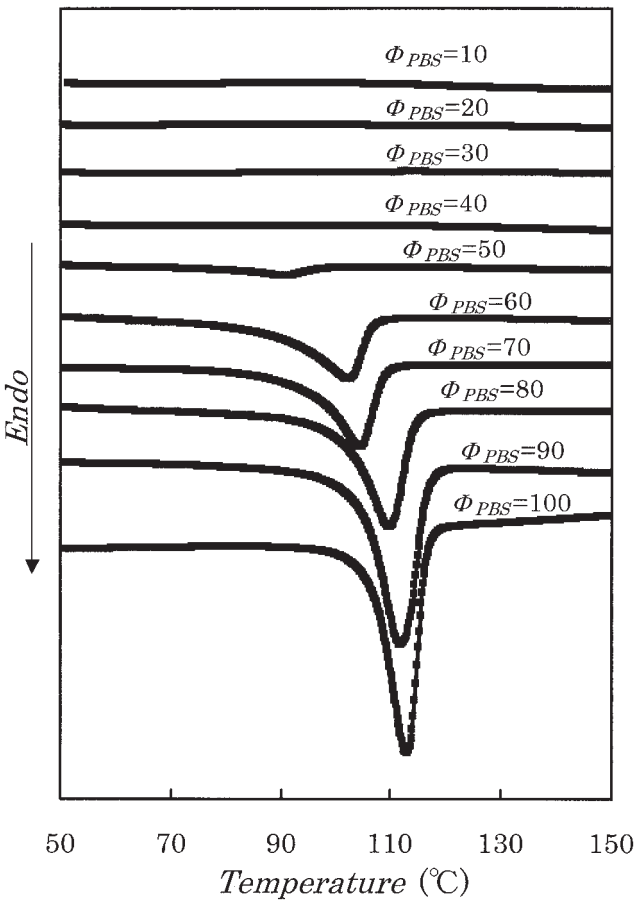

Figure 3 DSC curves of the blend films.

90% up to ϕ_{PBS} = 50. However, the transparency decreases to 10% at ϕ_{PBS} = 60 and greater. Furthermore, the transparency of the blends was not observed in the ϕ_{PBS} = 90 and 100 samples, because a macrophase separation occured in the ϕ_{PBS} = 90 sample, and the film is shrunk in the ϕ_{PBS} = 100 sample. It seems that the transparency of the blends was related to the miscibility of these polymers.

Figure 2 shows the X-ray diffraction intensity curves of the blends.[9–11] Two intensity maximums originating from PBS crystallites can be observed at about 2θ = 20° in the PBS-rich blend films. However, these maximums cannot be seen in the CAB-rich blend films. This means that PBS cannot form a crystalline structure, but PBS forms an amorphous structure in CAB-rich conditions. In the CAB-rich blend, broad intensity maximums were obtained near 2θ = 6 and 20°. This means that CAB is essentially amorphous, with small crystalline inclusions. These two maximums cannot be observed in the PBS-rich blend films.

Figure 3 shows the DSC curves of the blend films. Any peaks cannot be seen up to ϕ_{PBS} = 40. However, the endothermic peak, which corresponds to the melting point of PBS, can be observed at ϕ_{PBS} = 50 and greater. To discuss the effect of blend ratio on the melting behavior in detail, the value of the melting point, T_m, and the heat of fusion, ΔH_m, were evaluated from the peak position and peak area, respectively. The results are shown in Figure 4. A straight solid line was drawn through the values of ΔH_m at ϕ_{PBS} = 100 and ΔH_m at ϕ_{PBS} = 0, where the value for ΔH_m was 0 at ϕ_{PBS} = 0. The value of T_m and ΔH_m cannot be observed up to ϕ_{PBS} = 40. It can be seen that the T_m increases as ϕ_{PBS} increases in the range from ϕ_{PBS} = 50 to ϕ_{PBS} = 100. The T_m of the ϕ_{PBS} = 100 sample is about 10°C higher than that of ϕ_{PBS} = 50. There is a difference between the straight line and the plots; the

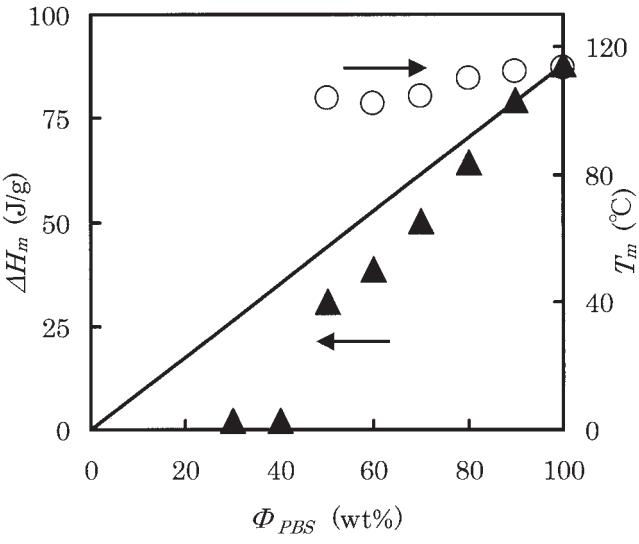

Figure 4 Effect of Φ_{PBS} on T_m and ΔH_m of the blend films.

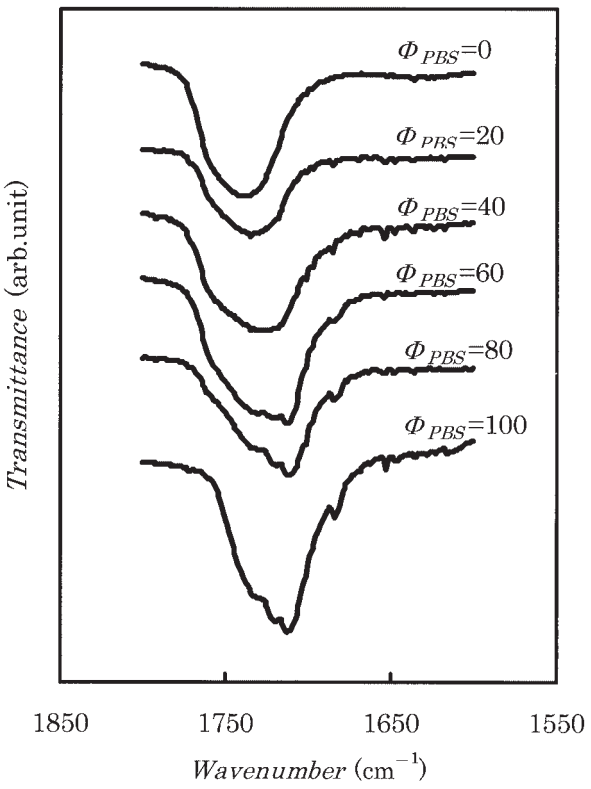

Figure 5 FT-IR curves of the blend films.

value of ΔH_m is not greater than the straight line. These results suggest that the CAB molecules inhibit crystallization of PBS in the blends and the PBS molecules are in an amorphous state when ϕ_{PBS} is low.

From the above results, it is found that homogenous blend films are obtained over a wide range of the blend ratio. Especially, over the range from $\phi_{PBS} = 0$ to $\phi_{PBS} = 30$, PBS molecules have a high miscibility with CAB molecules and PBS molecules are in an amorphous state. To gain insight with regard to the effect of interaction between the molecules on the blend structure, we examined each blend using infrared spectroscopy. Figure 5 shows the IR spectra of the blend films. There is a difference between the peak position of the carbonyl group of CAB and that of PBS. When there are significant interactions between the carbonyl group of CAB and that of PBS in the blend films, new peaks corresponding to the interaction should be observed. However, the blend films do not show any additional peaks. Therefore, this result suggests that there is no significant interaction between PBS and CAB. Hence, it seems that the strong interaction is not a main reason for the CAB molecule being miscible with the PBS molecule.

To probe the blend structure in more detail, we perform the dynamic mechanical analysis of the blends. Figure 6 shows the DMA curves of the blend films. The storage modulus, E', decreases as ϕ_{PBS} increases at about room temperature. It seems that the PBS molecules act as a lubricant in the blend films. The curves of loss modulus, E'', versus temperature indicate the peaks that correspond to the glass transition temperature, T_g. The peaks shown in the low temperature region may correspond to the T_g of PBS; the peaks shown in high temperature region may correspond to the T_g of CAB or the blend phase. To discuss the relation between the value of T_g and the blend ratio, the effect of ϕ_{PBS} on T_g was investigated. The results are shown in Figure 7. The line drawn in the graph was calculated by using the Fox equation.[12–14]

$$\frac{1}{T_{g\,CAB/PBS}} = \frac{W_{CAB}}{T_{g\,CAB}} + \frac{W_{PBS}}{T_{g\,PBS}}$$

where T_{gCAB} and T_{gPBS} denote the glass transition temperature of CAB and PBS, respectively. W_{CAB} and W_{PBS} denote the weight fraction of CAB and PBS, respectively. This equation proposes the theoretical value of $T_{gCAB/PBS}$ and the composition dependence of the glass transition in miscible polymer blend. In other

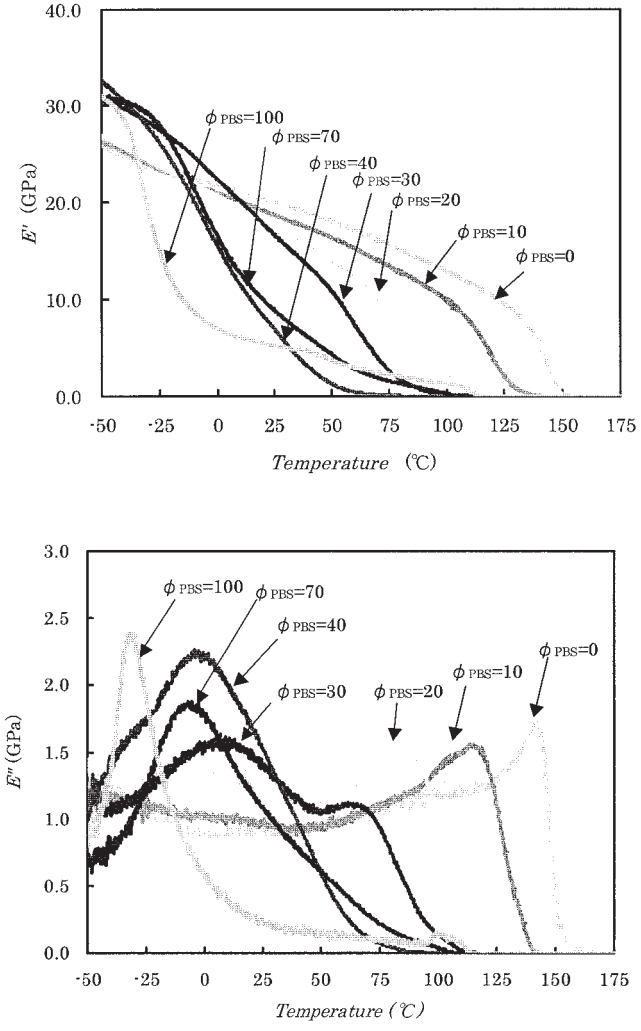

Figure 6 DMA curves of the blend films.

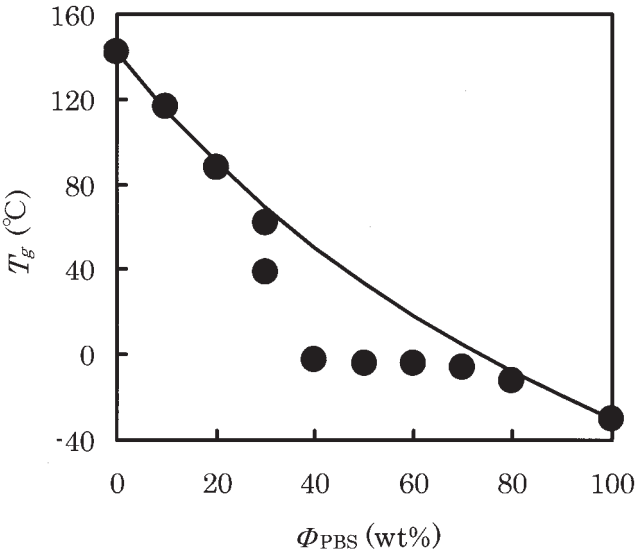

Figure 7 Effect of Φ_{PBS} on the T_g of the blend films.

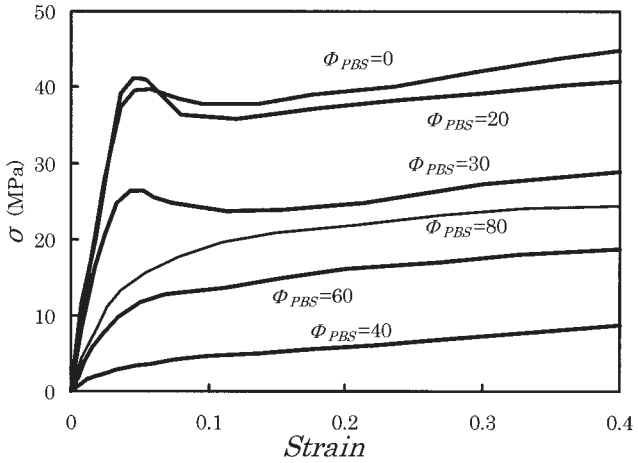

Figure 8 Stress–strain curves of the blend films.

words, miscible blends show a single T_g that equals $T_{gCAB/PBS}$, but immiscible blends show a separate T_g associated with each phase. The T_g of the blend films is in accord with the theoretical value of $T_{gCAB/PBS}$ in the range from $\phi_{PBS} = 0$ to $\phi_{PBS} = 30$, and the T_g decreases with the increase of ϕ_{PBS} because of a plasticization effect of the PBS molecule. Therefore, it seems that PBS molecules have a high miscibility with CAB molecules and PBS molecules are in an amorphous state over this composition range. However, the T_g of the blend films is in disaccord with theoretical value of $T_{gCAB/PBS}$ in the range from $\phi_{PBS} = 40$ to $\phi_{PBS} = 80$. These T_gs show nearly constant values located in approximately the same T_g of pure PBS. This result implies the presence of a pure amorphous region of PBS in the blend system. Moreover, it is noted that the DMA curve of $\phi_{PBS} = 30$ has two separate T_gs at about 10 and 80°C, which may be associated with the glass transition of the PBS phase and that of the CAB/PBS blend phase, respectively. Additionally, taking account of the result of the X-ray diffraction analysis and DSC, we conclude that PBS molecules form both crystalline and amorphous regions, and a portion of the amorphous PBS molecule is blended with a portion of the CAB molecules over the range from $\phi_{PBS} = 30$ to $\phi_{PBS} = 80$.

Figure 8 shows the stress–strain curves of the blend films. The yield stress of the blends decreases with the increase of ϕ_{PBS} up to $\phi_{PBS} = 40$, and it shows a minimum value at $\phi_{PBS} = 40$. The yield stress increases with the increase of ϕ_{PBS} at $\phi_{PBS} = 40$ and greater. Figure 9 shows the relation between Young's modulus, E, and the blend ratio. The value of E decreases as ϕ_{PBS} increases up to $\phi_{PBS} = 40$. The E then increases and shows almost the same value as the E of pure PBS at $\phi_{PBS} = 50$ and greater. When ϕ_{PBS} is low, it seems that the decrease of Young's modulus can be attributed to the plasticizing effect of PBS, which is in an amorphous state. When ϕ_{PBS} is high, PBS molecules form a crystalline structure. Because of this crystalline structure, it seems that the Young's modulus of the blend films increases a little bit with increasing ϕ_{PBS}.

Observation of porous material

Figure 10 shows the SEM images of the extracted and dried films. Pores could be observed both on the surface and internally in the $\phi_{PBS} = 30$ sample. However, pores could not be observed in the $\phi_{PBS} = 50$ and $\phi_{PBS} = 70$ samples. As mentioned above, the interaction between PBS and CAB is not strong. Therefore, when ϕ_{PBS} is low, a portion of CAB molecules is eluted from the blends. Since PBS would form continuous and three-dimensional networks, the blends are not de-

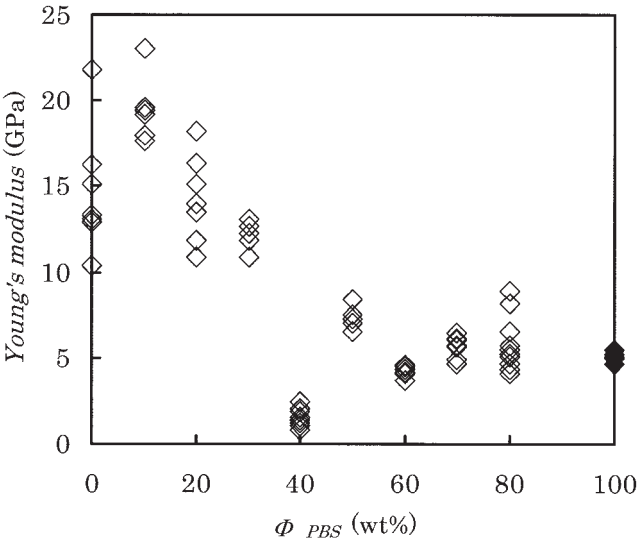

Figure 9 Effect of Φ_{PBS} on the Young's modulus of the blend films.

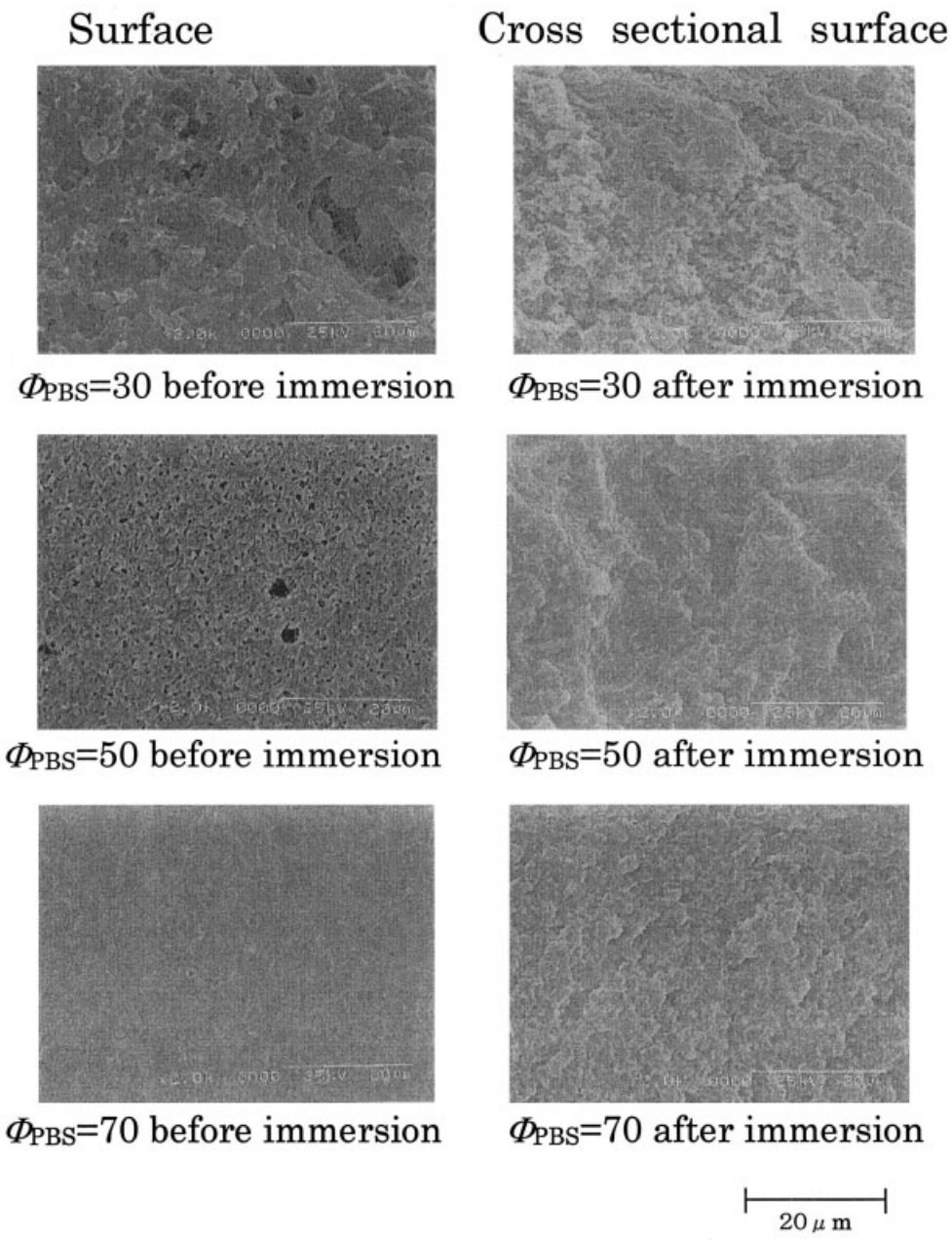

Figure 10 SEM micrographs of the blend films: before immersion in acetone and after immersion in acetone.

graded in acetone. It seems that the removal of the CAB molecule changes the structure of the blends and the pore structure might be produced. However, when ϕ_{PBS} is high, the small amount of CAB molecules is dispersed in the PBS matrix. Therefore, it seems that the CAB molecules could not be eluted from interior of the blend, and the pore structure could not be produced.

Figure 11 shows the DSC curves of the blend films immersed in acetone and the neat blend films. The DSC curve of the immersed film shows an endothermic peak at $\phi_{PBS} = 30$, even though the neat film does not show any endothermic peak. Moreover, the T_m value of the immersed blend film is higher than that of the neat film in the $\phi_{PBS} = 50$ sample; the peak area of the immersed blend film is larger than that of the neat blend film. This result implies that the degree of the crystallinity of PBS in the blend is increased by the immersion in acetone. It seems that the removal of the CAB molecule trapped in the blends allows the PBS molecules in the amorphous state to be crystallized. Additionally, this result also supports the idea that pore structure could be produced by the restructure of the blends with elution of CAB molecules.

Compatibility of cellulose ester/biodegradable aliphatic polymer blend films

Table I shows the compatibility of typical cellulose ester/biodegradable aliphatic polymer blend systems. CAB and CAP are miscible with all listed aliphatic polymers except for poly(L-lactic acid) (PLLA), and CTA (DS = 2.99) is only miscible with PBS. However, CA (DS = 1.52) is immiscible with all listed aliphatic polymers. This result suggests that the compatibility of cellulose ester is enhanced with the increase of DS and the size of ester substitutions. Additionally, it seems that the compatibility of the aliphatic polymer in the blend systems is improved as the number of methylene groups between carbonyl groups increases.

CONCLUSION

CAB/PBS blend films were obtained by using cast-blend method. We investigated the structure and physical properties and the following conclusions were deduced:

1. There is no marked interaction between the carbonyl group of PBS and that of CAB. Hence, it seems that significant interaction is not the main reason for the CAB molecule being miscible with the PBA molecule.
2. The CAB molecule inhibits crystallization of PBS in the blends, and PBS molecules are in an amorphous state when ϕ_{PBS} is low.
3. The Young's modulus of the blend films decreases as ϕ_{PBS} increase up to $\phi_{PBS} = 40$, because of the plasticizing effect of PBS. The Young's modulus shows almost the same value as that of pure PBS at $\phi_{PBS} = 40$ and greater.
4. Porous materials could be produced in the $\phi_{PBS} = 30$ sample by immersion the blend films in acetone.
5. The compatibility of the cellulose ester/biodegradable aliphatic polymer blend system is enhanced with an increase in DS and the size of ester substitutions of cellulose esters. Moreover, the compatibility of the blend systems is improved as the number of methylene groups of aliphatic polymers between carbonyl groups is increased.

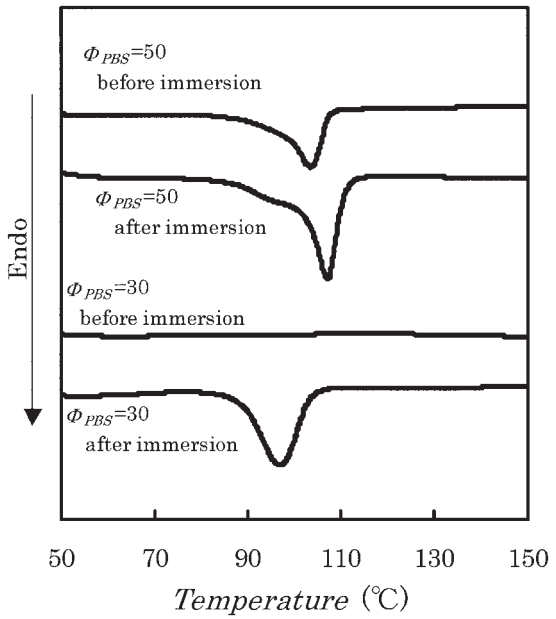

Figure 11 DSC curves of the blend films: before immersion in acetone and after immersion in acetone.

TABLE I
Compatibility of Aliphatic Polyesters and Cellulose Esters

Cellulose ester	Aliphatic polyesters			
	PBS	PCL	PHBV[a]	PLLA[b]
CA	×	×	×	×
CTA	○	×	×	×
CAB	○	○	○	×
CAP	○	○	○	×

○, Macroscopic phase separation is observed; ×, Macroscopic phase separation is not observed
[a] Poly(hydroxybutyrate *co* valerate).
[b] Poly(L-lactide).

References

1. Davé, V.; Glasser, W. G. Polymer 1997, 38, 2121.
2. El-Shafee, E.; Saad, G. R.; Sherif, M.; Fahmy Eur Polym J 2001, 37, 2091.
3. Maristella, S.; Giuseppina, C.; Maria, P. Macromolecule 1992, 25, 6441.
4. Nishio, Y.; Haratani, T.; Takahashi, T. Macromolecule 1989, 22, 2547.
5. Nishio, Y.; Matsuda, K.; Miyashita, Y.; Kimura, N.; Suzuki, H. Cellulose 1997, 4, 131.
6. Buchanan, C. M.; Gedon, S. C.; White, A. W.; Wood, M. D. Macromolecule 1992, 25, 7373.
7. Buchanan, C. M.; Gedon, S. C.; White, A. W.; Wood, M. D. Macromolecule 1993, 26, 5704.
8. Technical data sheet of Showa Highpolymer Co. Ltd., Tokyo, Japan.
9. Gert, Y. V.; Kozlov, P. V.; Bakeyev, N. F. Vysokomol Soedim 1975, 4, 887.
10. Stipanovic, J.; Sorko, A. Polymer 1978, 19, 3.
11. Iwata, T.; Okamura, K. Azuma, J. Cellulose 1996, 3, 91.
12. Fox, T. G.; Bill, A. Phys Soc 1956, 1, 123.
13. Eguiburu, J. L.; Iruin, J. J.; Fernandez-Berridi, M. J.; San Román, J. Polymer 1998, 39, 6891.
14. Jim, H. J.; Chin, I. J.; Kim, M. N.; Kim, S. H.; Yoon, J. S. Fahmy Eur Polym J 2000, 36, 165.